

# Synthesis of Multimetal–Graphene Composite by Mechanical Milling

BACHU SAIPHANEENDRA,<sup>1</sup> AVI KRISHNA SRIVASTAVA,<sup>1</sup>  
and CHANDAN SRIVASTAVA<sup>1,2</sup>

1.—Department of Materials Engineering, Indian Institute of Science, Bangalore 560012, India.

2.—e-mail: csrivastava@materials.iisc.ernet.in

Multimetal–graphene composites were synthesized using the ball milling technique. To prepare the composite, graphite powder was mixed with Fe, Cr, Co, Cu and Mg powders. This mixture was then mechanically milled for 35 h in toluene medium. After milling, the multimetal–graphite mixture was mixed with sodium lauryl sulfate and sonicated for 2 h. Sonication led to the exfoliation of graphene sheets. Formation of graphene was confirmed from x-ray diffraction and Raman spectroscopy. Transmission electron microscopy-based analysis revealed the formation of multimetal deposits over the graphene surface. Compositional analysis of the multimetal deposits revealed fairly uniform distribution of all the five component metal atoms over the graphene sheet. The average composition of the multimetal deposit was determined to be  $11.4 \pm 4$  at.% Mg,  $33.8 \pm 19$  at.% Cr,  $21.8 \pm 16$  at.% Fe,  $9.4 \pm 5.7$  at.% Co and  $23.6 \pm 12$  at.% Cu.

## INTRODUCTION

Graphene exhibits remarkable electronic,<sup>1</sup> optical<sup>2</sup> and mechanical properties.<sup>3</sup> Present research activities on graphene are extensively focused on designing and manufacturing materials and devices which, using novel functionalities offered by graphene, can be technologically exploited. One popular method is through graphene-based composites.<sup>4,5</sup> Graphene-based composites are typically of three kinds: (1) composites in which graphene is incorporated within a metal or a polymer matrix, (2) composites in which graphene sheets are sandwiched between different materials in a multilayer arrangement, and (3) composites in which nano-sized solids are grown over the graphene surface. Research on graphene-based composites is, however, typically restricted to single or bi-component metal–graphene systems. One possible way to enhance the properties and multifunctionality of graphene-based composites is to load graphene with multimetals. Multicomponent metallic alloys, commonly known as high entropy alloys, are already being extensively explored because of their remarkable properties.<sup>6,7</sup> The literature lacks reports on a unique graphene-based composite in which ultrafine multicomponent (five

or more metals) metallic deposits are decorating the graphene surface. Such a composite could offer multifunctionality due to individual and synergistic responses of the metallic components in the multimetal deposits to a stimulus while retaining the flexibility and strength of the graphene sheet. This is essential for applications such as ultrafine multifunctional coatings formed by spray coating of a multicomponent metal–graphene composite over a suitable substrate.

This paper describes the synthesis and characterization of multicomponent metal–graphene composites. The ball milling technique was used initially to form alloyed deposits of five different metals (Fe, Co, Cr, Cu and Mg) within the graphite lattice. A subsequent exfoliation of the multimetal–graphite composite by surfactant-assisted sonication produced graphene decorated with multimetal deposits. In addition to the excellent thermal and electrical conductivity of the graphene, the presence of the metal atoms (Mg, Cr, Fe, Co and Cu) in the multimetal–graphene composite will provide the following functionalities: Cr will enhance the corrosion resistance, Fe and Co will impart ferromagnetic property, Cu will enhance the conductivity, and Mg will provide light weight and high strength.

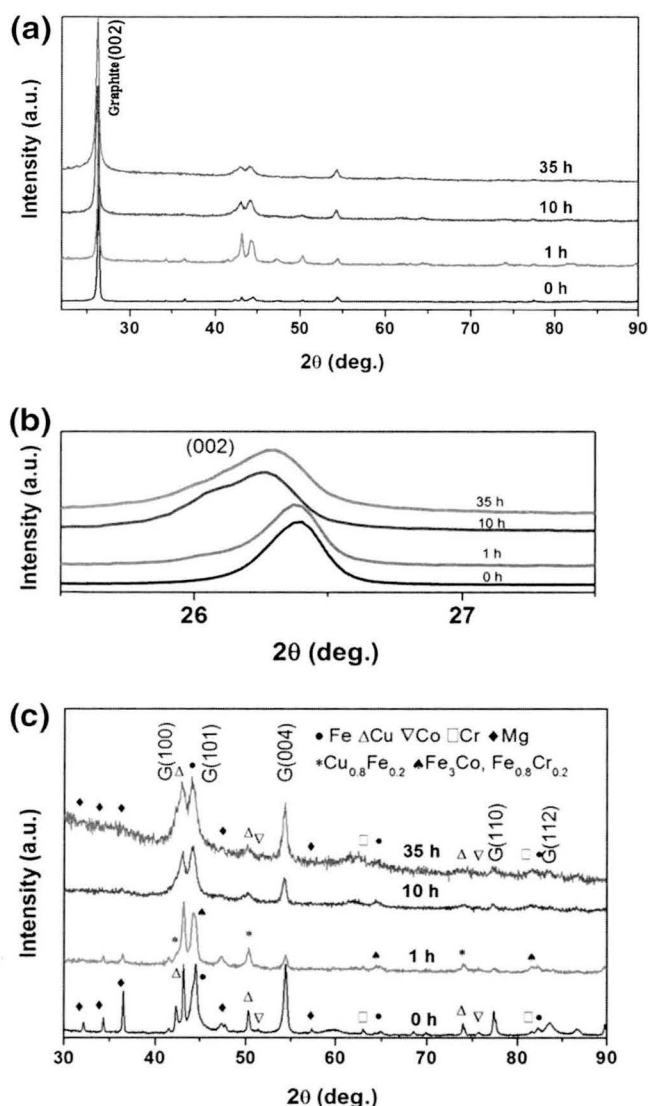


Fig. 1. (a) XRD profile obtained from as-mixed and milled samples, (b) XRD profile showing only the (002) peak of graphite and (c) XRD profile showing the peaks in the 2- $\theta$  range of 30–90°. The location of peaks corresponding to the pure metal atoms is also indicated for the 35-h milled sample.

## EXPERIMENT

The planetary ball mill used in the present study was manufactured by Eloquent Technologies, India. Initially, graphite rods weighing 8 g were ground in a mortar. The ground graphite was mixed with 0.439 g of iron (Fe), 0.408 g of chromium (Cr), 0.499 g of copper (Cu), 0.463 g of cobalt (Co) and 0.191 g of magnesium (Mg) powder. This graphite–metal mixture was then dropped into a high chromium steel vial of the ball mill containing stainless steel balls weighing approximately 200 g. Ball milling of the graphite and metal powder mixture was carried out in toluene medium up to 35 h at 300 rpm. After 35 h, 10 mg of the ball-milled sample was dispersed in 10 mL ethanol containing

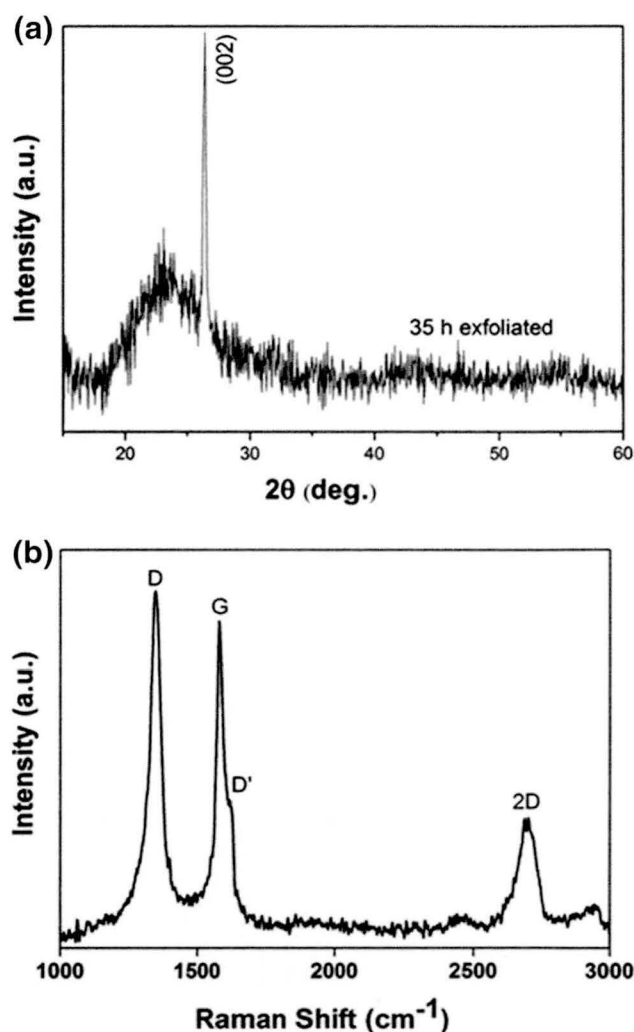


Fig. 2. (a) XRD pattern and (b) Raman spectrum obtained from SLS exfoliated 35-h milled sample.

20 mg sodium lauryl sulfate (SLS). This mixture was then sonicated for 2 h followed by centrifugation at 7500 rpm for 10 min to remove the SLS. The centrifuged precipitate was then dispersed in water and allowed to settle overnight. The resultant supernatant solution contained a stable dispersion of graphene which was then separated for further analysis.

X-ray diffraction (XRD) profiles from the as-synthesized samples were obtained by using a X-pert pro x-ray diffractometer employing a  $\text{CuK}_\alpha$  radiation ( $\lambda = 0.1540$  nm) source. Average composition of the milled sample was obtained using the energy dispersive spectroscopy (EDS) technique with an ESEM Quanta 200 scanning electron microscope (SEM) operating at 20 kV. The Raman spectrum from the exfoliated sample was obtained using a microscope set-up (HORIBA JOBIN–YVON, Lab RAM HR) consisting of a diode-pumped solid-state laser operating at 532 nm with a charge-coupled detector. A 300-kV field emission FEI Tecnai F-30 transmission

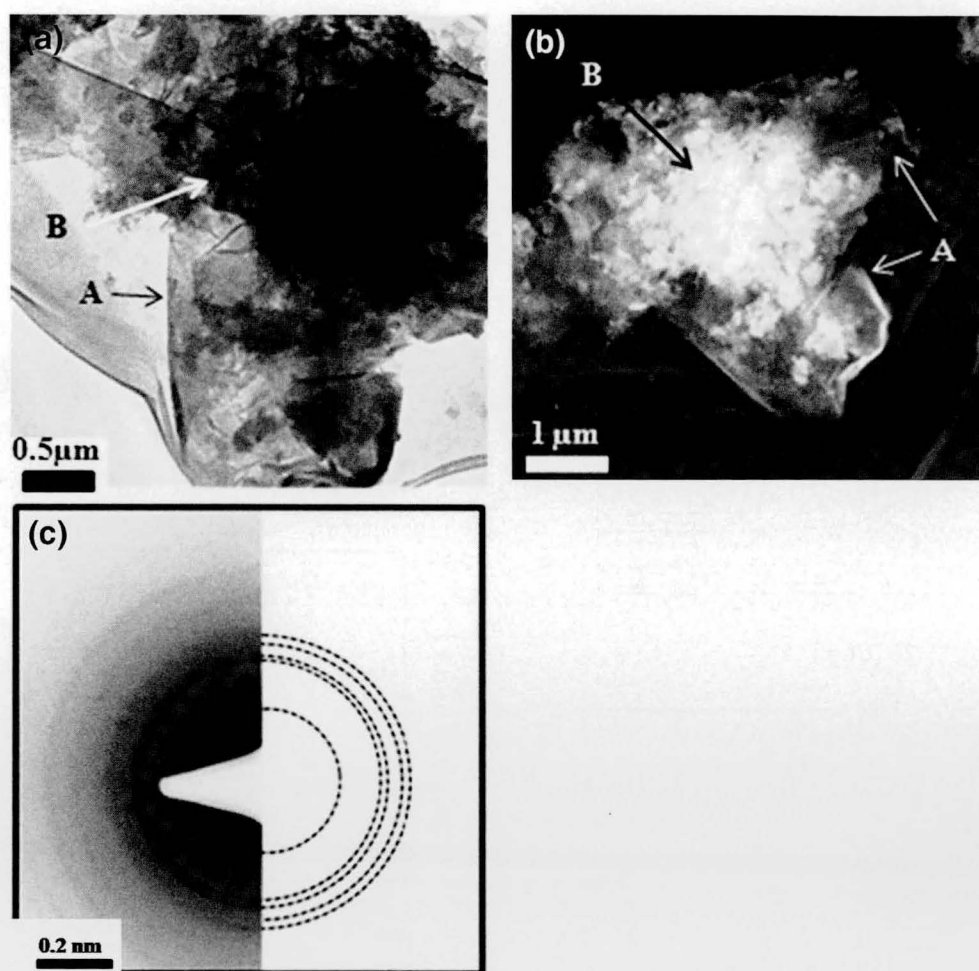


Fig. 3. Representative (a) TEM (b) STEM-HAADF, and (c) SAD patterns obtained from multimetal-graphene composite. The dashed lines in the SAD pattern are added for ease of viewing of the faint diffraction rings. Graphene sheet is marked A and the metal deposit is marked B in both micrographs.

electron microscope (TEM) was used for obtaining TEM bright field images and selected area electron diffraction (SAD) patterns from the as-synthesized samples. Samples for the TEM-based analysis were prepared by drop-drying the as-synthesized samples onto a carbon-coated nickel grid. The scanning transmission electron microscopy-energy dispersive spectroscopy (STEM-EDS) technique was used for the compositional mapping and compositional line profile analysis of the as-synthesized samples. For the STEM-EDS analysis, the samples were imaged using a high-angle annular dark field (HAADF) detector in the STEM mode.

## RESULTS AND DISCUSSION

XRD profiles obtained from the as-mixed powders and samples milled for 1 h, 10 h and 35 h are provided in Fig. 1a. The XRD profile in Fig. 1b derived from Fig. 1a shows only the (002) XRD peak of the graphite. The XRD profile in Fig. 1c, again derived from Fig. 1a, shows the XRD profile for the

2-theta angle range of 30°–90°. In Fig. 1b, the shift of the XRD peak to a low 2-theta value with the increase in milling time reveals an increase in the interplanar spacing of the (002) graphitic planes with milling. This can be due to the incorporation of the metal atoms within the graphite interplanar spacing during milling. In Fig. 1c, the XRD profile obtained from the as-mixed sample shows peaks corresponding to the pure metals added to the vials. As the milling progresses, intermetallic compounds such as  $\text{Fe}_3\text{Co}$ ,  $\text{Fe}_{0.8}\text{Cr}_{0.2}$  and  $\text{Cu}_{0.8}\text{Fe}_{0.2}$  form at intermediate stages of milling, as revealed by the peaks in the XRD profile obtained from the 1-h milled sample. With the increase in the milling time to 35 h, the XRD peaks corresponding to the pure metals and intermetallic phases disappear. This indicates the formation of ultra-fine multimetallic clusters within the graphite inter-planar spacings. The absence of metal oxide peaks indicates minimal oxidation (if any) during milling. The absence of oxidation during the milling process can be attributed to the presence of toluene during the milling.<sup>8</sup>

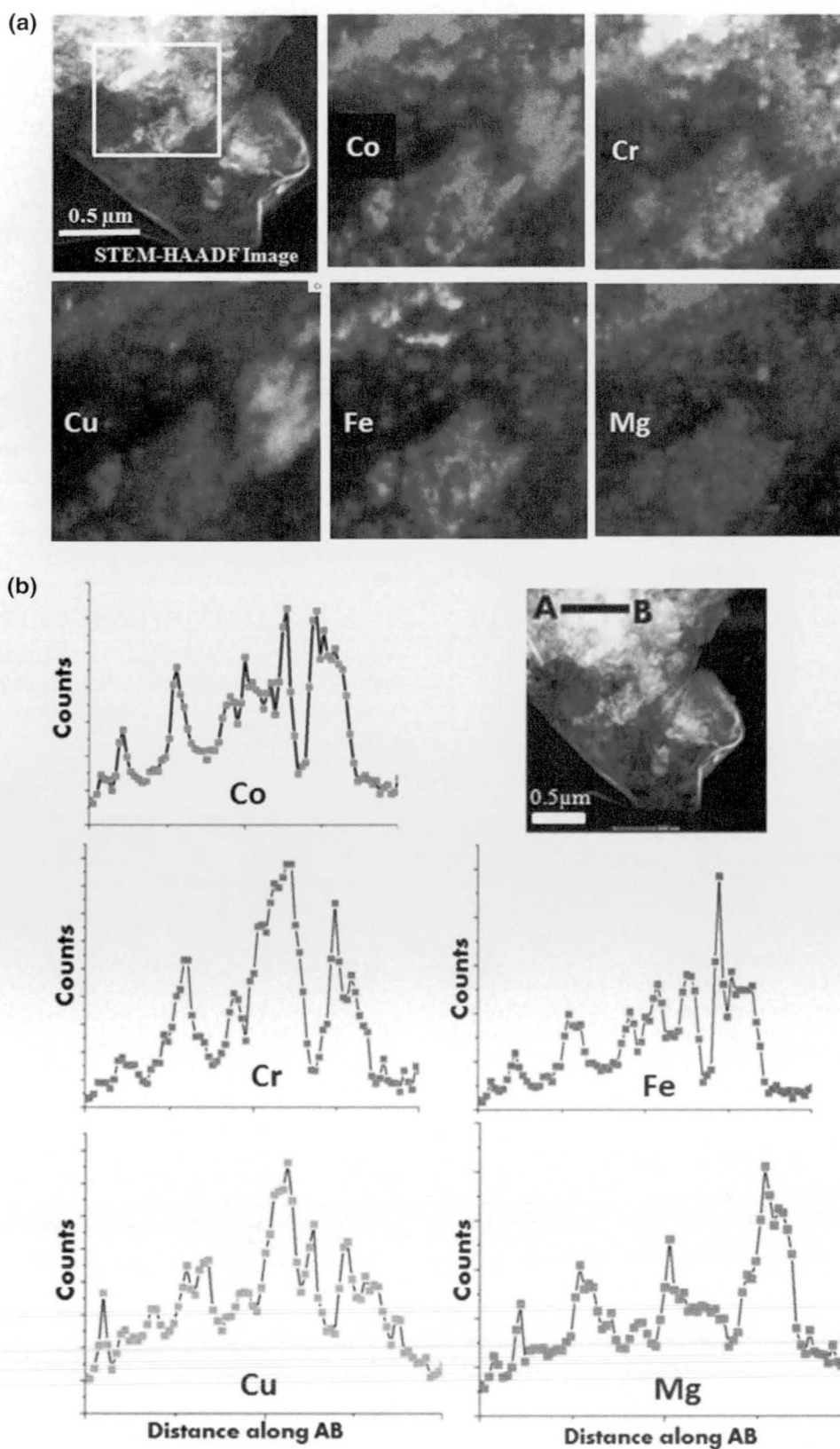


Fig. 4. (a) Representative compositional mapping result obtained from a region of interest, and (b) representative compositional line profile analysis result obtained from an individual nanoparticle.



The XRD profile obtained from the SLS exfoliated samples milled for 35 h is shown in Fig. 2a. It shows a broad hump around  $23.18^\circ$  2-theta with an overlapping sharp peak at  $26.44^\circ$  2-theta, indicating the presence of graphene in the exfoliated sample.<sup>9</sup> The Raman spectrum of SLS exfoliated 35-h ball-milled sample in Fig. 2b shows three bands: D, G and 2D at around  $1347\text{ cm}^{-1}$ ,  $1581\text{ cm}^{-1}$  and  $2700\text{ cm}^{-1}$ , respectively, which are characteristic of graphene.<sup>9</sup> In a typical sample, the D band corresponds to  $sp^3$  defects, the G band corresponds to in-plane vibrations of  $sp^2$  carbon atoms and the 2D band corresponds to two phonon lattice vibrations.<sup>10</sup>

The SEM-EDS compositional analysis performed on the 35-h milled sample revealed the composition of the multimetal-graphene composite to be  $11.4 \pm 4\text{ at.}\%$  Mg,  $33.8 \pm 19\text{ at.}\%$  Cr,  $21.8 \pm 16\text{ at.}\%$  Fe,  $9.4 \pm 5.7\text{ at.}\%$  Co and  $23.6 \pm 12\text{ at.}\%$  Cu. The SEM-EDS data reveal an appreciable distribution in composition between different regions in the multimetal-graphene composite. The composite contains regions that are rich in Cr, Fe and Cu.

The TEM bright field image and STEM-HAADF image obtained from the SLS exfoliated 35-h milled sample showing the presence of metal deposits over the graphene sheet is provided, respectively, in Fig. 3a and b. The graphene sheet is marked 'A' and the metal deposit is marked 'B' in both micrographs. A representative SAD pattern obtained from the graphene-metal composite is shown in Fig. 3c. The SAD pattern exhibits sharp rings revealing the crystallinity of the multimetal deposits. The SAD pattern does not show any diffraction signature corresponding to pure elemental phases or their oxides. This indicates the alloying of the component metal atoms in the composite.

The STEM-EDS compositional profile and compositional mapping analysis were used to determine the uniformity in the distribution of the component metal atoms in the multimetal-graphene composite. The results obtained from the compositional mapping experiment are provided in Fig. 4a and b. The compositional mapping analysis qualitatively revealed uniformity in the distribution of the component metals atoms in the multimetal-graphene composite. The result obtained from the compositional line profile experiment is shown in Fig. 4a

and b. The line profile analysis confirmed the co-presence of all the five metal atoms at every analysis point. The line profile analysis, however, also revealed a non-uniform distribution of the component metal atoms in the multimetal-graphene composite.

## CONCLUSION

Mechanical milling of Fe, Cr, Co, Cu and Mg metal powders with graphite and then subsequent chemical exfoliation of the 35-h milled sample composite in which multimetal deposits formed over the graphene sheets. Diffraction-based analysis of the composite indicated towards the formation of alloys between the component metal atoms. The electron diffraction pattern did not reveal any diffraction signature corresponding to pure metal phase or their oxide phases. Compositional analysis of the composite revealed a non-uniform distribution of the component metal atoms within the multimetal deposits formed over the graphene surface.

## ACKNOWLEDGEMENTS

Authors acknowledge the electron microscopy facilities in the AFMM, IISc Bangalore. Research funding from SERB, Government of India is also acknowledged.

## REFERENCES

1. A.H. Castro Neto, F. Guinea, N.M.R. Peres, K.S. Novoselov, and A.K. Geim, *Rev. Mod. Phys.* 81, 109 (2009).
2. F. Bonaccorso, Z. Sun, T. Hasan, and A.C. Ferrari, *Nat. Photon.* 4, 611 (2010).
3. I.A. Ovidco, *Rev. Adv. Mater. Sci.* 34, 1 (2013).
4. X. Huang, X. Qi, F. Boeyab, and H. Zhang, *Chem. Soc. Rev.* 42, 666 (2012).
5. S. Stankovich, D.A. Dikin, G.H.B. Dommett, K.M. Kohlhass, E.J. Zimney, E.A. Stach, R.D. Piner, S.T. Nguyen, and R.S. Ruoff, *Nature* 442, 282 (2006).
6. Y. Zhang, T.T. Zuo, Z. Tang, M.C. Gao, K.A. Dahmen, P.K. Liaw, and Z.P. Lu, *Prog. Mater. Sci.* 61, 1 (2014).
7. J.W. Yeh, S.K. Chen, S.J. Lin, J.Y. Gan, T.S. Chin, T.T. Shun, C.H. Tsau, and S.Y. Chang, *Adv. Eng. Mater.* 6, 299 (2004).
8. X. Xu, J.H. Kim, W.K. Yeoh, Y. Zhang, and S.X. Dou, *Supercond. Sci. Technol.* 19, L47 (2006).
9. M. Alanyalioglu, J.J. Segura, J.O. Sole, and N.C. Pastor, *Carbon* 50, 142 (2012).
10. M.K. Punith Kumar, S. Shanthini, and C. Srivastava, *RSC Adv.* 5, 53865 (2015).